A Comparative Study of Light Emitting Diodes based on All-Inorganic Perovskite Nanoparticles ($CsPbBr_3$) Synthesized at Room Temperature and by Hot Injection Method

Bruno ClasenHames,[†] Rafael Sánchez Sánchez,[§]AzharFakharuddin,[†,‖]Iván Mora Seró[†]*

[†]Institute of Advanced Materials (INAM), UniversitatJaume I, 12071 Castelló, Spain

[§]Department of Chemistry, University of Liverpool, Crown St., L69 3BX, Liverpool, United Kingdom

[‖]Department of Physics, University of Konstanz, 78457 Konstanz, Germany

*corresponding author I.M.S.: sero@uji.es

Abstract: Perovskite nanoparticles (PeNPs) have been extensively studied for optoelectronic applications due to their extremely high photoluminescence quantum yield, tunable bandgap, and exceptionally narrow emission spectra. Therefore, PeNPsare considered excellent candidates for the development of high efficiency, low-cost, wide gamut and high purity color displays. However, their synthesis typically involves multi-step cumbersome processes that might hinder its commercial development. In this work, we reportgreen light-emitting diodes (LEDs) prepared using all inorganic PeNPs $CsPbBr_3$ synthesized at room temperature (RT) and compare their performance with those prepared by a traditional hot injection (HI) method.We provide insights into the morphology, optoelectronic properties of RT PeNPs via atomic force and transmission electron microscopy and employing them in LEDs.

Keywords: Perovskite, LED, $CsPbBr_3$, Hot injection, Room Temperature

TOC:

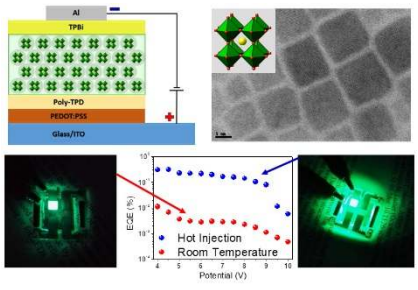

We have synthesized perovskite nanoparticles (PeNPs) through two different procedures, e.g., hot injection (HI) and a room temperature synthesis (RT). The light-emitting diodes (LEDs) prepared using the two types of PeNPs show superior performance for HI PeNPs. The morphology and optoelectronic investigations revealed that the HI PeNPs are characterized by a lower thin film surface roughness, narrow size distribution, and a higher radiative yield that is responsible for the higher performance.

Introduction

All inorganic perovskite nanoparticles with the general formula $CsPbX_3$ ($X = Cl^-, Br^-, I^-$) have gained attention in the scientific community due to their outstanding optoelectronic properties, such as the extremelyhigh photoluminescence quantum yield(as high as90 %), narrowemission spectra(FWMH ≈ 12 - 42 nm),tunablebandgap depending on the particle size and composition, low preparation cost, and abundance of precursor materials.[1–4]Since theiremergencein 2014,PeNPs have been considered an excellent candidate as primary semiconductor in photodetectors,[5] light-emittingelectrochemical cells,[6]photochemical conversion,[7] solar cells,[8,9] lasers,[10] and light-emitting diodes.[11–16] The particularly interesting optoelectronic characteristics of PeNPs make thisfamily of materials anexceptionalalternativefor the development of unprecedented high quality full color displays.

In just two years of research, LEDs based on PeNPs synthesized by the HI method have reached external quantum efficiencies (EQEs)beyond8%,[17] which is an outstanding achievementcompared to other technologies. Nowadays, the cadmium-based quantum dots (Cd-QDs) LEDs, thathave been extensively investigated during the last two decades, show state of art EQE ~20.5% for red LEDs.[18,19]Nonetheless, there are some limiting factors that hinders its industrial application for quotidian purposes. On one hand, Cd-QDs employ hazardous elements such asCd theirsynthesis, on the other hand,requires relatively high temperature, controlled atmosphere to avoid undesired oxidation reactions,use of expensive raw materials, and most importantly,sophisticated core/shell structures in order to reach high PLQY.

Soon after the first report of organic-inorganic hybrid PeNPs by Perez-Prieto and coworkers,[20]Kovalenko and coworkers synthesized,[1] for the first time, all-inorganic PeNPs via a hot injection method – a method that requires high temperature. However, a more recent low temperature compatible synthesis is reported in 2016.[21]The new methodology exploits a supersaturated recrystallization method, which transfers the Cs^+, Pb^{2+} and the X^- ions dissolved in DMF to a non-polar solvent (toluene)at room temperature. Surprisingly, these PeNPs also presented PLQY values above 90%. This new method simplifies significantly the synthesis ofthe semiconductor nanocrystals withoutthe need of high temperatures or controlled atmosphere. Despite the relative simplicity of the synthetic method and outstanding optical properties of the nanocrystals, their application in an optoelectronic device is not yet reported.

A crucial parameter to be taken into account towards the preparation of high efficiencyLEDsbased on PeNPs is the careful removalof excess organic solvents and surfactants present in the crude solution whichare essential for a proper nucleation and controlled crystallization.Therefore,great attention must be paid on the purification process of the nanoparticles, which wouldotherwise decrease the PLQY or evenlead to PeNPsaggregation and subsequent precipitation.Swarnkarand coworkers recently developed a purification methodusing

methylacetate (MeOAc), an antisolvent that removes the excessnon-volatile solvents and reagentswithout inducing agglomeration.[8]Li and coworkersdemonstrated the preparation of LEDs with high efficiency from solution-processed $CsPbBr_3$ nanoparticlesthrough balancing surface passivation and carrier injection via ligand density control using hexane/ethyl acetate mixed solvent.[15] Despite the growing research progress in PeNPs, the stability of colloidal solutions and stable device lifetime are yet to be demonstrated.

In this work, we reportfor the first time the preparation ofgreen LEDs using $CsPbBr_3$ PeNPssynthesized at RT as a light-emitting material, which could be an important step forward from the industrial point of view, taking into account the simplicity of the synthetic method. We note that the RT PeNPs demonstrate an inferior performance due to relatively poorer size distribution, and perhaps due to the fact that no further purification was applied to it, compared to the HI PeNPs, where a solvent purification led to improved NP morphology.

Results and Discussion

Green light-emitting $CsPbBr_3$ PeNPshave been prepared throughtwo different methods (see experimental section for further details). We usethe HI method, previously reported in literature to yield suitable PeNPs for the preparation of LEDs to compare the optoelectronic properties ofRT PeNPs. Both methodologies produced $CsPbBr_3$ NPs with cubic structure as determined by X-ray diffraction, see Figure S1 in the Supporting Information. Figure 1 shows the absorbance andphotoluminescence (PL) spectra measured for the PeNPs prepared through the two different approaches.The RT nanoparticles exhibit a PLQY of 49 % (solution) and 15 % (film), whose emission maximum(λ_{em}^{max}) is centered at 509 nm and the PL spectrumshows a FWHM of 29 nm;whereas,theHI PeNPs showed a PLQY of 60%(solution) and 20 % (film) and the emission peak is centered at 514 nm (FWHM 28 nm). In both cases, the PL spectra are situated within the green spectral region with a slight bathochromic shift of 5 nm for the PeNPs synthesized through the HI method.This red-shiftbetween the PL emission peaks of the two PeNPsis due to the purification performed on HIPeNPsas proposed by Li *et. al.*[15] In fact, we note a similar red-shift for HI PeNPs before and after purification (see Figure S2).

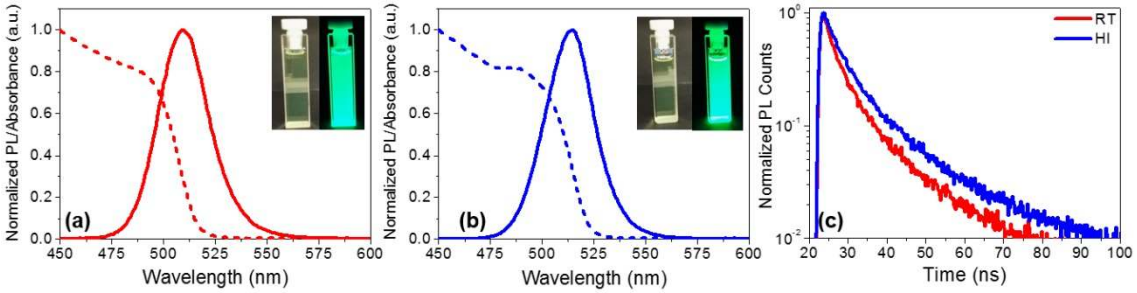

Figure 1. Absorbance (dashed line) and PL (solid line) spectra of the green light-emitting $CsPbBr_3$PeNPs synthesized (a) at RT and (b) by the HI method. The PL spectra were measured using the λ_{exc} = 440 nm for both nanoparticles. The insets show the solutions under white light and under UV light. (c) Transient PL decay curves for the RT (red) and HI (blue) PeNPs.

The Stokes shift observed in Figure 1(a) and Figure 1(b) for both types of PeNPsis also very similar, being ≈ 105 meV (21 nm) and ≈ 118 meV (24 nm) for the RT and HI, respectively.CdSe/CdS, CdSe/CdPbS and CdSe/CdZnS quantum dots typically show Stoke shift values of ≈ 400 meV, which aresignificantly larger than those observedfor PeNPs.[22]The smaller Stokes shifts observed here imply that the PL of the PeNPs arises from the direct exciton recombination process, which is in good agreement with previous reports.[23,24]Theabsorbance onsetof the PeNPs prepared at RT starts 525 nm while that observed for theHI PeNPsstarts at 531 nm. From the absorbance spectrum, it is possible to estimate the optical bandgap of the two types of PeNPs by using the Tauc plot, see Figure S3. The calculated bandgap match closely, e.g., 2.40 eV and 2.37eV for RT and HI method, respectively, as shown in Figure S3.[25] These results are in a good agreement with previous reports that have been used as a reference to this work.[11,21] Figure 1(c) show the transient PL decay for both types of PeNPs(in solution). Although a distinction between slow and fast decay that is typically ascribed to non-radiative and radiative processes, respectively, is hard to make a quantitative analysis of the two shows larger non-radiative lifetime for HI PeNPs. As recently reported by Tress a longer non radiative lifetime (or a higher radiative yield) leads to higher internal quantum efficiency (IQE).[26]

Figures 2(a) and 2(b) show the high-resolution transmission electron microscopy images (HR-TEM) of the RT and HI PeNPs, respectively. The bothPeNPs show size distribution with values below 20 nm and well-defined crystalline planes for both types of nanoparticles.However, we clearly observe that the geometry for the two types of PeNPs studied is significantly different, being more rectangular for the RT nanocrystals and more square for the nanocrystals synthesized through the HI method.The PL spectra of the PeNPswere transformed into the corresponding chromaticity indexes and plotted in the CIE 1931 color space chromaticity diagram. As shown in Figure 2(c), the red dot (0.057,0.642) and the blue dot (0.068,0.696) represent those chromaticity indexes corresponding to the PL spectra of the RT

and HI PeNPs, respectively; the proximity of the CIE values to the curve edge indicates the pure color nature of the emitted light.

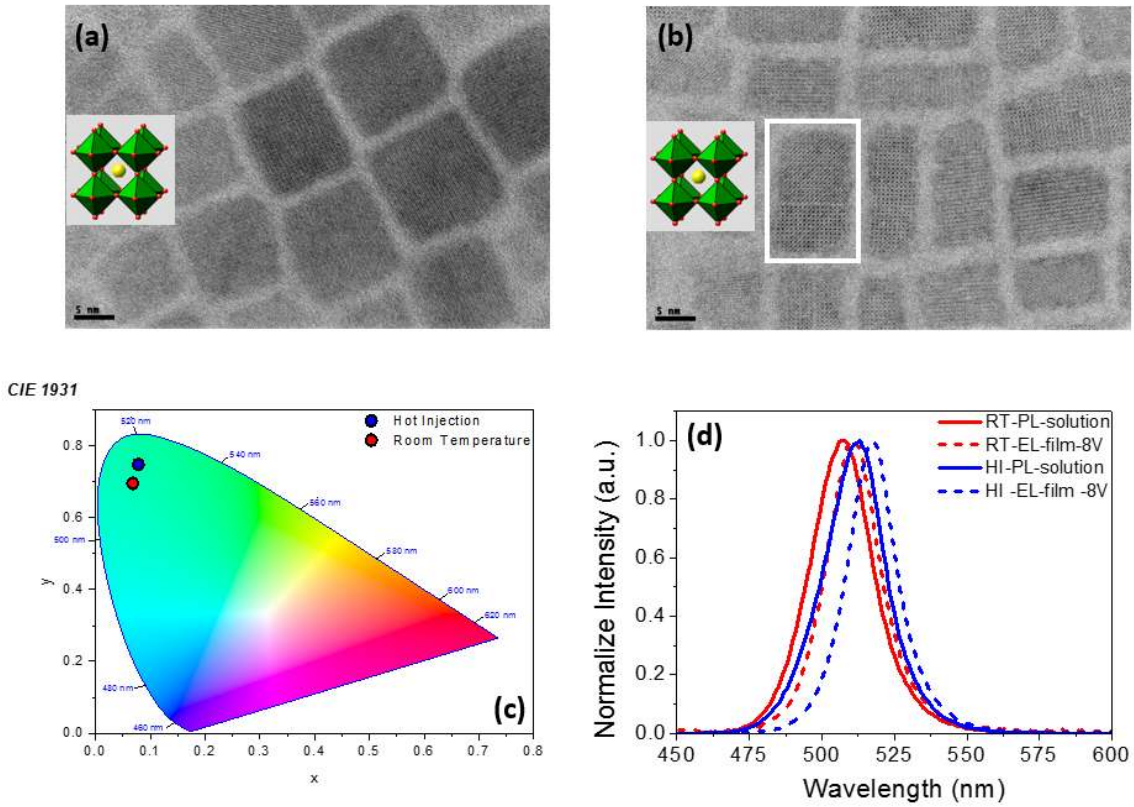

Figure 2. HR-TEM images of the (a) RT and (b) HI PeNPs nanocrystals. White rectangle in (b) encircles defective NPs. (c) Chromaticity indexes corresponding to the PL spectra for the RT (red) and HI (blue) PeNPs plotted in the CIE 1931 diagram; and (d) PL in solution (slid lines) using hexane as solvent and the EL spectra (dashed lines) of the PeNPs synthesized at RT and by HI method.

Figure 2(d) shows the PL spectra (in solution) and the electroluminescence (EL) spectra of a complete device (8V) for the PeNPs synthesized at RT and by HI method. A small red-shift between PL of NPs in solution and EL from PeNPs layers is evident for both kinds of NPs. The red-shift in the spectra (for EL) could be explained by the so-called Stark effect, e.g., the red-shift in presence of high electric field. Also the fact that recombination of hot electrons, which are present due to the applied bias, is not the same as in the case of PL, radiative recombination in a steady-state, and may lead to such a spectral shift.[27]

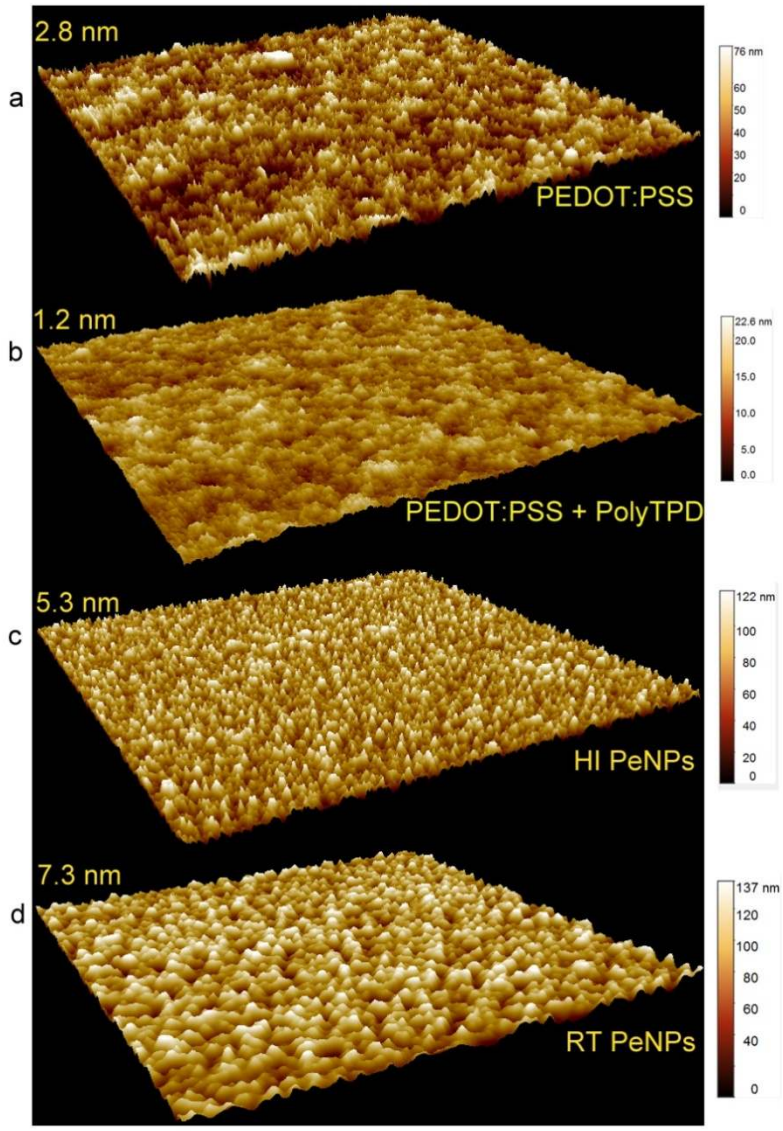

Figure 3. AFM images of PEDOT:PSS (a), PEDOT:PSS with a thin layer of Poly-TPD on top (b), HI PeNPs (c) and RT PeNPs (d) deposited on top of a PEDOT/Poly-TPD layer. The r.m.s. roughness is marked on top left of each image. The scan area is 10 μm × 10 μm.

In order to determine the surface coverage and surface roughness of the films, we recorded topography of as deposited films using atomic force microscopy (AFM) on relatively large area (10 μm × 10 μm). The root mean square roughness calculated for PEDOT was 2.8 nm, which reduced to 1.2 nm when a thin layer of Poly-TPD is deposited on top suggesting formation of a smoother film (Figure 3(b)). The HI PeNPs showed a smaller r.m.s. roughness value (5.3 nm) compared to RT PeNPs (7.3 nm) suggesting that the former leads to a smooth film formation probably due to a narrow size distribution and smaller particle size. A lower surface roughness and narrow size distribution are prerequisites to high performing devices. Furthermore, the RT method leads to formation of small clusters with the film which might hinder the device performance.

We employed both kinds of nanocrystals an absorber material forLEDs, see experimental section. Figure 4(a)depicts energy level diagram of the materials employedfor the complete devices, while Figure 4(b) and Figure 4(c)shows a photograph of the green LED at 8 V prepared at RT and by HI, respectively.EL spectra at different applied voltage are depicted in Figure S4.All the devices were prepared using ITO as the substrate, a thin layer of PEDOT:PSS as a hole transport material on top of the ITO, then a poly-TPD layer as an electron blocking layer, followed by the deposition of thePeNPsand aTPBi layer as an electron transport material. Tofinally complete the devices,the thermal evaporation of aluminum electrodes was carried out.

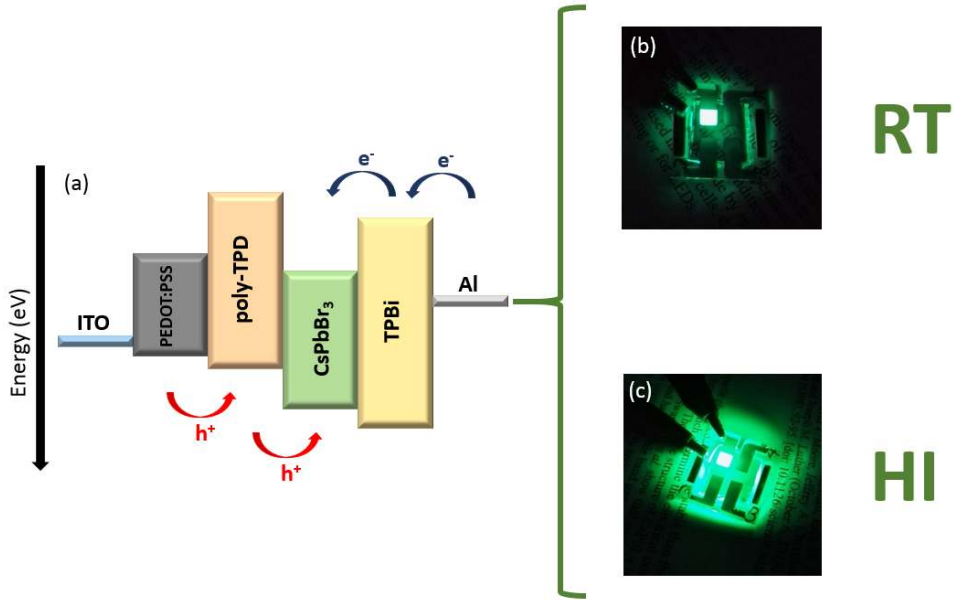

Figure 4.(a) Energy diagram of the materials employed for the preparation of the PeNPs-LEDs. Bright green LEDs driven at 8 Volts, using PeNPs prepared at (b) RT and (c) by HI method.

The performances of the LEDs prepared with both PeNPswas studied. Figure 5shows the electro-optical response of the LEDs prepared with the RT and HI PeNPs, respectively. Figure 5(a) shows the current density of both kinds ofPeNPs. Devices prepared withPeNPssynthesized through the HI method show lower current at low applied voltages. At voltages between 8 and 9 Volts both devices exhibit similar current densities. However, at voltages beyond 9 V, the HI particles show higher current density values. These variations probably arisefrom the different synthesis procedures (the HI involves high temperature synthesis and a subsequent purification that yield a high quality PeNPs), see the experimental section.Figure 5(b) reveals significant variations of the current efficiency values depending on the PeNPsemployed. The higher PLQY and the lower currents contributeto the observed higher efficiency for HI LEDs. The maximum current efficiency value was observed was 0.7 $Cd \cdot A^{-1}$, which correspond to those devices prepared from the HI method particles. The data plotted in Figure 5(c) show that the maximum luminance values range from 303.2 $Cd \cdot m^{-2}$ for HI and 2.66 $Cd \cdot m^{-2}$ for RT PeNPs, respectively.

Consequently, the maximum EQE values range from 0.31 % for the HI and 0.01% for the RTPeNPs. It is worth highlighting that all the devices show turn-on voltages at around 4 Volts regardless of the type of PeNPs employed and all the devices were measured from 4 to 10 V.

The clear difference in EQE of both kinds of nanoparticles, see Figure 5(d), where HI PeNPs exhibit a superior performance,can be attributed to several factors. The first concerns the synthesis process, the PeNPs synthesized by the HI method provide PeNPs with higher quality than those prepared at RT.Different factors could contribute to this result, on the one hand HI PeNPs presented a narrower size distribution, see Figure 2(a) and Figure 2(b),avoiding that small variations in the bandgap act as traps reducing the performance of the LEDs.On the other hand, the rectangular shape of PeNPs prepared at RT probably arises from the merging of different NPsand defects at the boundary between the original particles can be formed, see for example the NP encircled by a white rectangle in Figure 2(b).The higher radiative yield of theHIPeNPs (a ratio between non-radiative and radiative recombination) is another reason for their high performance (see the Figure 1(c)). The lowerPLQY or the particles synthesized at RT compared to the ones prepared through the HI method also points to a higher degree of lattice defectsfor the RT PeNPs. Moreover, the purification method also introduces differences between both systems, being the second factor affecting the lower performance of devices prepared with RT nanoparticles. In a single synthesis exploiting the HI method, it is possible to prepare a larger amount of material and apply some purification processes to remove excess organic solvents, which is not possible with the synthesis at room temperature since the amount of material obtained after each synthesis is relatively small. Finally the lower roughness of HI PeNPs also favor the higher performance of this kind of nanoparticles.

It must be noted that the devices stability is still a question as both the LEDs starts to degrade at an applied bias 8 V see Figure S5, as also evident from a sudden drop in EQE (Figure 5(d)). However, the stability of these devices is in the scope of our future works and will be explained in details in our upcoming reports.

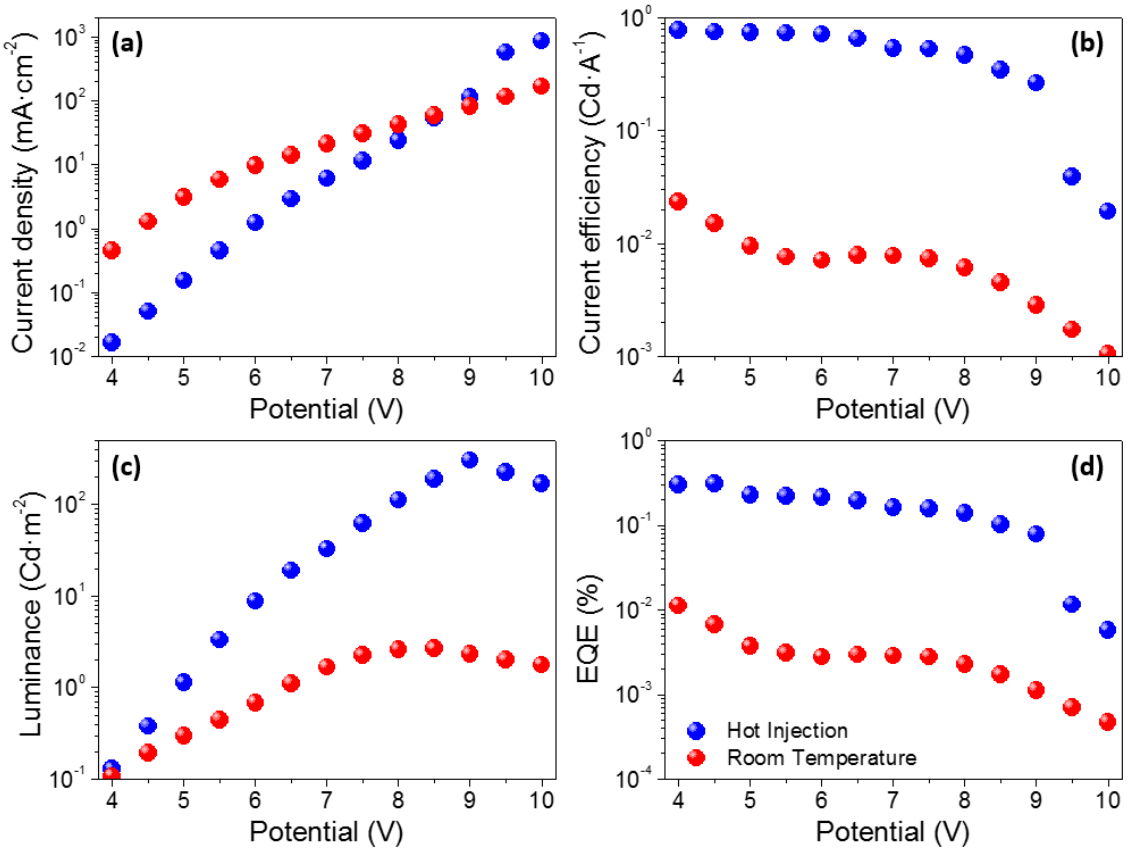

Figure 5. Analysis of the QD-LED performance: (a) current density curves (*J/V*), (b) current efficiency, (c) luminance and (d) EQE.

CONCLUSIONS

In summary, we have synthesized the perovskite nanoparticles (PeNPs) through two differentprocedures, e.g., hot injection (HI) and a room temperature synthesis (RT). The light-emitting diodes (LEDs) prepared using the twotypes of PeNPsshowsuperior performancefor HI PeNPs.The morphology and optoelectronic investigations revealed that the HI PeNPs are characterized by a lower thin film surface roughness, narrow size distribution, and a higher radiative yield that is responsible for the higher performance. Although the LED EQE efficiency of the RT PeNPs is lower, their facile and large scale compatible offer potential for mass production. A further improvement in the performance using RT PeNPscould be made via a control over particle size distribution and their further purification.

Experimental Section

All the materials employed in this work were used as received from the commercial suppliers and were used directly without further purification. Those precursors and solvents employed for

the PeNPs synthesis were purchased from Sigma Aldrich. Oleic acid (90 %), Oleylamine (≥ 98 %) 1-Octadecene (90 %), Hexane (≥ 97 %), Toluene (99.8 %) Methyl acetate (99.5 %), N,N-Dimethylformamide (99.8%), Cesium bromide (99.999 %), Cesium carbonate (99.995 %). Lead(II) Bromide were purchased from TCI. The pre-patterned ITO substrates (20x20 mm) were purchased from Thin Film Devices (TFD), PEDOT:PSS (Al4083) from HeraeusClevios and, Poly[N,N'-bis(4-butylphenyl)-N,N'-bisphenylbenzidine] (poly-TPD) (M_n 100,000-150,000) from Ossila and 2,2′,2"-(1,3,5-Benzinetriyl)-tris(1-phenyl-1-H-benzimidazole) (TPBi) were acquired from Sigma Aldrich.

Hot Injection Method

Preparation of Cs-oleate: Cs_2CO_3 (0.814g) was loaded into 100 mL 3-neck flask along with octadecene (40mL, Sigma-Aldrich, 90%) and oleic acid (2.5 mL, OA, Sigma-Aldrich, 90%), dried for 1h at 120 °C, and then heated under N_2 to 150 °C until all Cs_2CO_3 reacted with OA. Since Cs-oleate precipitates out of ODE at roomtemperature, it has to be pre-heated to 100 °C before injection.

Synthesis of $CsPbBr_3$ NCs: ODE (10 mL) and $PbBr_2$ (0.138g) were loaded into 50 mL 3-neck flask and dried under vacuum for 1h at 120 °C. Dried oleylamine (1.0 mL, OLA) and dried OA (1.0 mL) were injected at 120 °C under N_2. After complete solubilization of a $PbBr_2$ salt, the temperature was raised to 180 °C and Cs-oleate solution (0.8 mL, 0.125 M in ODE, prepared as described above) was quickly injected and, 5s later, the reaction mixture was cooled by the ice-water bath.[1]

Purification of $CsPbBr_3$ NCs: The crude solution was cooled down with water bath and aggregated NCs were separated by centrifuging and removing as many solvents as possible involved in the synthesis process. Thereafter, after discarding the supernatant,thePeNPsweredispersed in hexane to only apply the purification process with MeOAc in the ratio of (1:3). ThePeNPswere centrifuged for 10 min at 4,700 r.p.m. After that, they weredispersed again in hexane and stored at low temperature for 48h to precipitate Pb-oleate and Cs-oleate which solidify and precipitate at low temperatures. After this periodthePeNPs were separated to the precipitatedmaterial. The solutions stored in the fridge are stables for months.

Room Temperature Method: To synthesized the $CsPbBr_3$, was necessary $PbBr_2$ (0.4 mmol) and CsBr (0.4 mmol) dissolved in DMF (10 mL). When the precursors were totally solved, OA (1.0 mL) and OLA (0.5 mL) are added to stabilize the precursor solution. Then, 1.0 mL of the precursor solution was added drop by drop into toluene (10 mL) under vigorous stirring. Strong green emission was observed immediately after the injection.[21] The solutions stored in the fridge are stables for months.

Purification of $CsPbX_3$ NCs: After the synthesis of the PeNPs, each solution was centrifuged during 10 min at 4,700 r.p.m. The supernatantwas discarded and the solid wasdispersed in hexane. After that, all the material was placed in the same flask which was kept at low temperatures for 48 h. The precipitated material was removed and the final solution was concentrated to 10 $mg \cdot ml^{-1}$.

Preparation of the NPs-based light-emitting diodes: The ITO substrates were introduced in a soap solution and sonicated for 30 min. Then the substrates were firstly rinsed with Mili-Q water and secondly with ethanol. Next, the ITO substrates were introduced in a mixture of solvents consisting of isopropanol:acetone (1:1 *v/v*) and sonicated for 30 min. After that, the substrates were rinsed with ethanol and dried with compressed air. Then, the substrates were introduced in a UV-O_3 cleaner for 30 min and the PEDOT:PSS solution was spun-cast at 3,000 r.p.m. during 60 s and treated at 150 °C for 30 min in air, to yield a thin layer (20 nm). Next, a poly-TPD layer (20 nm) was deposited by spin-casting (10 $mg \cdot ml^{-1}$in chlorobenzene) at 3,000 r.p.m. for 60 s and subsequently annealed at 150 °C for 30 min in air. After that, the PeNPs solutions (10 $mg \cdot ml^{-1}$) in hexane were spun-cast at 2,000 r.p.m. during 20 s. Finally, a 20 nm of TPBi and a 100 nm aluminum top electrode was thermally evaporated at a rate of 0.5 $Å \cdot s^{-1}$ and 1.5-2 $Å \cdot s^{-1}$ respectively; the active areas were encapsulated with adhesivetape and after that with a UV photo-curable epoxy resin from Lighting Enterprises (ELC4908-30) and a cover glass.

Characterization equipment: The absorbance spectra were registered with a UV/VIS Varian Cary 300 BIO spectrophotometer and for the PL spectra fluorometer from Horiba Fluorolog 3-11were used. The performance of the LEDs (*J/V* curves, EL spectra, current efficiency, luminance and EQE) was quantified with an external quantum efficiency measurement system C9920-12 from Hamamatsu, based on an integrating sphere connected to a PMA-12 Photonic multi-channel detector through an optical fiber and using a Keithley 2400 as a current/voltage source meter.The photoluminescence quantum yield was measured with an absolute PL Quantum Yield measurement system with monochromatic light source C9920-02, -03 from Hamamatsu, connected to an integrating sphere.The high resolution transmission electronic microscopy (HR-TEM) images of the QDs were registered with a JEOL 2100 microscope.Time-resolvedemissionmeasurements were done with the technique of time correlated single photon counting (TCSPC) in an IBH-5000U apparatus. Samples were excited with a 464 nm NanoLED with a FWHM of 1.4 ns and a repetition rate of 100 kHz. Atomic force microscopy (Concept Scientific Instrument) was employed to probe surface roughness of the deposited films.

Acknowledgment.The work was supported by MINECO of Spain (project MAT2016-76892-C3-1-R). B.C.H is grateful to the support of the National Council of Technological and Scientific Development (CNPq), Brazil, through the Science without Borders program. A.F. acknowledge Alexander von Humboldt Foundation for the postdoctoral fellowship.

References

1. Protesescu, L. *et al.* Nanocrystals of Cesium Lead Halide Perovskites (CsPbX3, X = Cl, Br, and I): Novel Optoelectronic Materials Showing Bright Emission with Wide Color Gamut. *Nano Lett.***15,** 3692–3696 (2015).

2. Song, J. *et al.* Quantum Dot Light-Emitting Diodes Based on Inorganic Perovskite Cesium Lead Halides (CsPbX3). *Adv. Mater.***27,** 7162–7167 (2015).

3. Zhang, X. *et al.* Bright Perovskite Nanocrystal Films for Efficient Light-Emitting Devices. *J. Phys. Chem. Lett.***7,** 4602–4610 (2016).

4. Ling, Y. *et al.* Bright light-emitting diodes based on organometal halide perovskite nanoplatelets. *Adv. Mater.***28,** 305–311 (2016).

5. Ramasamy, P. *et al.* All-inorganic cesium lead halide perovskite nanocrystals for photodetector applications. *Chem. Commun.***52,** 2067–2070 (2016).

6. Aygüler, M. F. *et al.* Light-Emitting Electrochemical Cells Based on Hybrid Lead Halide Perovskite Nanoparticles. *J. Phys. Chem. C***119,** 12047–12054 (2015).

7. Xu, Y.-F. *et al.* A CsPbBr3 Perovskite Quantum Dot/Graphene Oxide Composite for Photocatalytic CO2 Reduction. *J. Am. Chem. Soc.***139,** 5660–5663 (2017).

8. Swarnkar, A. *et al.* Quantum dot–induced phase stabilization of α-CsPbI3 perovskite for high-efficiency photovoltaics. *Science (80-.).***354,** 92 LP-95 (2016).

9. Sidhik, S. *et al.* Enhanced Photovoltaic Performance of Mesoscopic Perovskite Solar Cells by Controlling the Interaction between CH3NH3PbI3 Films and CsPbX3 Perovskite Nanoparticles. *J. Phys. Chem. C***121,** 4239–4245 (2017).

10. Wang, Y. et al. Solution-Processed Low Threshold Vertical Cavity Surface Emitting Lasers from All-Inorganic Perovskite Nanocrystals. *Adv. Funct. Mater.***27,** 1–7 (2017).

11. Zhang, X. *et al.* Enhancing the Brightness of Cesium Lead Halide Perovskite Nanocrystal Based Green Light-Emitting Devices through the Interface Engineering with

Perfluorinated Ionomer. *Nano Lett.***16,** 1415–1420 (2016).

12. Huang, H. *et al.* Polyhedral Oligomeric Silsesquioxane Enhances the Brightness of Perovskite Nanocrystal-Based Green Light-Emitting Devices. *J. Phys. Chem. Lett.***7,** 4398–4404 (2016).

13. Li, G. *et al.* Highly Efficient Perovskite Nanocrystal Light-Emitting Diodes Enabled by a Universal Crosslinking Method. *Adv. Mater.***28,** 3528–3534 (2016).

14. Shan, Q. *et al.* All-inorganic quantum-dot light-emitting diodes based on perovskite emitters with low turn-on voltage and high humidity stability. *J. Mater. Chem. C***5,** 4565–4570 (2017).

15. Li, J. *et al.* 50-Fold EQE Improvement up to 6.27% of Solution-Processed All-Inorganic Perovskite CsPbBr3 QLEDs via Surface Ligand Density Control. *Adv. Mater.***29,** (2017).

16. Li, G. *et al.* Efficient Light-Emitting Diodes Based on Nanocrystalline Perovskite in a Dielectric Polymer Matrix. *Nano Lett.***15,** 2640–2644 (2015).

17. Chiba, T. *et al.* High-Efficiency Perovskite Quantum-Dot Light-Emitting Devices by Effective Washing Process and Interfacial Energy Level Alignment. *ACS Appl. Mater. Interfaces***9,** 18054–18060 (2017).

18. Jing, P. *et al.* Vacuum-free transparent quantum dot light-emitting diodes with silver nanowire cathode. *Sci. Rep.***5,** 12499 (2015).

19. Dai, X. *et al.* Solution-processed, high-performance light-emitting diodes based on quantum dots. *Nature***515,** 96–99 (2014).

20. Schmidt, L. C. *et al.* Nontemplate Synthesis of CH3NH3PbBr3 Perovskite Nanoparticles. *J. Am. Chem. Soc.***136,** 850–853 (2014).

21. Li, X. *et al.* CsPbX3 Quantum Dots for Lighting and Displays: Room Temperature Synthesis, Photoluminescence Superiorities, Underlying Origins and White Light-Emitting Diodes. *Adv. Funct. Mater.***26,** 2435–2445 (2016).

22. Zhao, H. et al. Perovskite quantum dots integrated in large-area luminescent solar concentrators. *Nano Energy***37,** 214–223 (2017).

23. Peng, L. et al. Size-controlled synthesis of highly luminescent organometal halide perovskite quantum dots. *J. Alloys Compd.***687,** 506–513 (2016).

24. Zhang, F. et al. Brightly Luminescent and Color-Tunable Colloidal CH3NH3PbX3 (X = Br, I, Cl) Quantum Dots: Potential Alternatives for Display Technology. *ACS Nano***9,**

4533–4542 (2015).

25. Eom, K. et al. Depth-resolved band alignments of perovskite solar cells with significant interfacial effects. *J. Mater. Chem. A* **5,** 2563–2571 (2017).

26. Tress, W. Perovskite Solar Cells on the Way to Their Radiative Efficiency Limit–Insights Into a Success Story of High Open-Circuit Voltage and Low Recombination. *Adv. Energy Mater.* (2017).

27. Henisch, H. K. Electroluminescence. *Reports Prog. Phys.* **27,** 369 (1964).